Ann. Henri Poincaré 11 (2010), 565–584

1424-0637/10/040565-20
published online June 8, 2010
DOI 10.1007/s00023-010-0035-6

Annales Henri Poincaré

Topological Graph Polynomials in Colored Group Field Theory

Razvan Gurau

Abstract. In this paper, we analyze the open Feynman graphs of the Colored Group Field Theory introduced in Gurau (Colored group field theory, arXiv:0907.2582 [hep-th]). We define the boundary graph $\mathcal{G}_\partial$ of an open graph $\mathcal{G}$ and prove it is a cellular complex. Using this structure we generalize the topological (Bollobás–Riordan) Tutte polynomials associated to (ribbon) graphs to topological polynomials adapted to Colored Group Field Theory graphs in arbitrary dimension.

1. Introduction

Discrete structures over finite sets, in particular graphs, are paramount to our present understanding of physics. Since Feynman realized that the perturbation series of quantum field theory is indexed by subclasses of graphs, the best experimentally tested physical predictions we have to this date rely solely on them.

Different quantum field theories generate different classes of graphs. The scalar Φ^4 field theory generates graphs formed of four valent vertices and lines. More involved quantum field theories, like Yang-Mills gauge theories [2,3], require further structure to be added (new particles, space-time indices, etc.). Random matrix models [4–7] and non commutative quantum field theories [8,9] generate ribbon graphs. A striking feature of the random matrix models and non commutative quantum field theories [10–14] is that the graphs are organized hierarchically. That is, the dominant contribution to the partition function is given by planar graphs, first order corrections are given by genus one graphs, second order corrections by genus two graphs, etc.

Random matrix models are relevant to very diverse physical and mathematical questions ranging from two dimensional quantum gravity to knot theory and quark confinement [15]. In the context of non commutative quantum field theory the topological power counting of the ribbon graphs has been shown in a series of papers to lead to a non trivial fixed point of the

renormalization group flow [16–20]. One can therefore expect that an appropriate generalization of such models to higher dimensions should also pose non trivial renormalization fixed points. The study of such generalizations holds essential clues for problems ranging from the quantization of gravity in higher dimensions to condensed matter.

Random matrix models generalize in higher dimensions to random tensor models, or group field theories (GFT) [21–23]. The perturbative development of such theories generates "stranded graphs [24].". The connection between GFTs and quantum gravity has been largely investigated [25]. Different models have been considered [26–29], and their semiclassical limit analyzed [30,31]. The study of the renormalization properties of such models has been started [32–34]. However, classical GFT models generate many singular graphs (that is graphs whose dual topological spaces have extended singularities). In a previous paper [1] we proposed a solution to this problem in the form of the "colored group field theory" (CGFT). The singular graphs are absent in this context in any dimension and the surviving graphs possess a cellular complex structure.

In this paper, we extend the study started in [1] of the Feynman graphs of the CGFT to open graphs (that is graphs with external half lines). For every such graph $\mathcal{G}$ we define its boundary graph $\mathcal{G}_\partial$. We prove that $\mathcal{G}_\partial$ has a cellular structure inherited from the graph $\mathcal{G}$. Extending the definition of the boundary operator of [1], we introduce the homology of $\mathcal{G}_\partial$ and explore some of its properties. Our model has been further studied in [35].

A simple and yet powerful way to encode information about a graph is through topological polynomials. Introduced first by Kirchhoff [36] they were studied (much) later by Tutte [37] as the solution of an inductive contraction deletion equation. The topological polynomials appear naturally in the dimensional regularization of quantum field theories [38] or in the study of statistical physics models [39–41]. The Tutte polynomials have been generalized by Bollobás and Riordan [42–45] to ribbon graphs. Further generalizations of these polynomials, respecting more involved induction equations, have been put in relation with the Feynman amplitudes of random matrix models and non commutative quantum field theories [46–49].

Relying on the cellular complex structure of $\mathcal{G}$ and $\mathcal{G}_\partial$ we propose a generalization of the classical topological polynomials adapted to CGFT graphs. These polynomials respect a contraction deletion equation and encode information about the cellular homology of the CGFT graph.

This paper is organized as follows. In Sect. 2 we briefly review the classical Tutte and Bollobás–Riordan polynomials. In Sect. 3 we detail the GFT graphs and define the boundary cellular complex and cellular homology for open graphs. In Sect. 4 we define the topological polynomials of CGFT graphs and show that they obey a contraction deletion relation. Section 6 draws the conclusions of our work.

The mathematics and physics nomenclature for graphs is very different and sometimes quite confusing. The reader is strongly encouraged to consult [49] for a dictionary. Also, some familiarity with ribbon graphs is assumed.

Again [49] (specifically Sections 4.1 and 4.3) provides a very good and concise introduction to this topic.

2. Tutte and Bollobás–Riordan Polynomials

This section is a short introduction to topological graph polynomials, see [49] and references therein for more detailed presentations.

A graph $\mathcal{G}$ is defined by the sets of its vertices $\mathcal{V}(\mathcal{G})$ and lines $\mathcal{L}(\mathcal{G})$. A line, connecting the vertices $v_1, v_2 \in \mathcal{V}(\mathcal{G})$ is denoted $l_{v_1 v_2} \in \mathcal{L}(\mathcal{G})$. For any line $l_{v_1 v_2}$ of $\mathcal{G}$ one can define two additional graphs[1]

- The graph with the line $l_{v_1 v_2}$ *deleted*, denoted $\mathcal{G} - l_{v_1 v_2}$, with set of lines $\mathcal{L}(\mathcal{G} - l_{v_1 v_2}) = \mathcal{L}(\mathcal{G}) \backslash \{l_{v_1 v_2}\}$ and set of vertices $\mathcal{V}(\mathcal{G} - l_{v_1 v_2}) = \mathcal{V}(\mathcal{G})$.
- The graph with the line $l_{v_1 v_2}$ *contracted*, denoted $\mathcal{G}/l_{v_1 v_2}$, is the graph obtained from $\mathcal{G}$ by deleting $l_{v_1 v_2}$ and identifying the two end vertices v_1 and v_2. That is $\mathcal{L}(\mathcal{G}/l_{v_1 v_2}) = [\mathcal{L}(\mathcal{G}) \backslash \{l_{v_1 v_2}\}]/(v_1 \sim v_2)$, $\mathcal{V}(\mathcal{G}/l_{v_1 v_2}) = \mathcal{V}(\mathcal{G})/(v_1 \sim v_2)$.
  Note that if $v_1 = v_2$ the $\mathcal{G}/l_{v_1 v_2} = \mathcal{G} - l_{v_1 v_2}$.

Given a graph $\mathcal{G}$ one can consider the family of its subgraphs. $\mathcal{H}$ is a subgraph of $\mathcal{G}$ (denoted $\mathcal{H} \subset \mathcal{G}$) if $\mathcal{V}(\mathcal{H}) = \mathcal{V}(\mathcal{G})$ and $\mathcal{L}(\mathcal{H}) \subset \mathcal{L}(\mathcal{G})$. Thus $\mathcal{G} - l_{v_1 v_2}$ is a subgraph of $\mathcal{G}$, whereas $\mathcal{G}/l_{v_1 v_2}$ is not.

The multivariate Tutte polynomial $Z_{\mathcal{G}}(q, \{\beta\})$ of the graph $\mathcal{G}$ depends on one variable $\beta_{l_{v_1 v_2}}$ associated to each line $l_{v_1 v_2}$ and an unique variable q counting the connected components of $\mathcal{G}$

Definition 1 (*Sum over subgraphs*).

$$Z_{\mathcal{G}}(q, \{\beta\}) = \sum_{\mathcal{H} \subset \mathcal{G}} q^{|k(\mathcal{H})|} \prod_{l_{v_1 v_2} \in \mathcal{L}(\mathcal{H})} \beta_{l_{v_1 v_2}}, \tag{1}$$

where $k(\mathcal{H})$ is the number of connected components of the subgraph $\mathcal{H}$.

This polynomial obeys a contraction deletion equation

Lemma 1. *For any line* $l_{v_1 v_2} \in \mathcal{L}(\mathcal{G})$,

$$Z_{\mathcal{G}}(q, \{\beta\}) = \beta_{l_{v_1 v_2}} Z_{\mathcal{G}/l_{v_1 v_2}}(q, \{\beta\} \backslash \{\beta_{l_{v_1 v_2}}\}) + Z_{\mathcal{G} - l_{v_1 v_2}}(q, \{\beta\} \backslash \{\beta_{l_{v_1 v_2}}\}). \tag{2}$$

For a graphs with no lines but with v *vertices* $Z_{\mathcal{G}}(q, \emptyset) = q^v$.

In quantum field theory one deals with graphs whose vertices are furthermore decorated with "half lines", or external legs.[2] We use halflines to encode information about the graph $\mathcal{G}$ in a subgraph $\mathcal{H}$. We will *always* replace a line belonging to $\mathcal{G}$ but not to $\mathcal{H}$ by two halflines on its end vertices.

[1] The two end vertices might coincide, $v_1 = v_2$.
[2] Or flags in the mathematical literature.

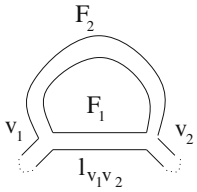

FIGURE 1. Ribbon vertices, ribbon lines and strands

The Tutte polynomial can be generalized to ribbon graphs. A typical ribbon graph with half lines is presented in Fig. 1. It is made of ribbon vertices (v_1 and v_2 in Fig. 1) and ribbon lines ($l_{v_1v_2}$ in Fig. 1). The lines and half lines in a ribbon graph have two sides, also called *strands*, represented by solid lines in Fig. 1.

The strands of a graph encode an extra structure. Tracing a strand one encounters one of the two cases

- Either one does *not* encounter a half line (F_1 in Fig. 1). In this case the closed strand defines an *internal face*.
- Or one *does* encounter a half line (F_2 in Fig. 1). In this case one continues on the second strand of this external half line (one "pinches" the external half line). The strands thus traced define an *external face*.
  This "pinching" is represented by the dotted curves in Fig. 1.

A ribbon subgraph $\mathcal{H} \subset \mathcal{G}$ of the ribbon graph $\mathcal{G}$ has the same set of vertices $\mathcal{V}(\mathcal{H}) = \mathcal{V}(\mathcal{G})$, but only a subset of the lines $\mathcal{L}(\mathcal{H}) \subset \mathcal{L}(\mathcal{G})$. Again, for a subgraph $\mathcal{H}$ all lines $l_{v_1v_2} \in \mathcal{L}(\mathcal{G})\backslash\mathcal{L}(\mathcal{H})$ are replaced by *pinched* external half lines. Thus, all internal faces of $\mathcal{H}$ are internal faces of $\mathcal{G}$, but there might exist external faces of $\mathcal{H}$ consisting of the union of pieces belonging to several internal faces of $\mathcal{G}$.

We are now in position to generalize the Definition 1 to ribbon graphs. We introduce an extra variable z counting *all* the faces (internal or external) of the graph, and define

Definition 2. The multivariate Bollobás–Riordan polynomial of a ribbon graph, analog to the multivariate polynomial of Eq. (1), is:

$$V_{\mathcal{G}}(q,\{\beta_l\},z) = \sum_{\mathcal{H}\subset\mathcal{G}} q^{k(\mathcal{H})} \left(\prod_{l_{v_1v_2}\in\mathcal{L}(\mathcal{H})} \beta_{l_{v_1v_2}} \right) z^{F(\mathcal{H})}, \tag{3}$$

where $k(\mathcal{H})$ is again the number of connected components of $\mathcal{H}$, and $F(\mathcal{H})$ the total number of faces.

The deletion of a ribbon line $l_{v_1v_2}$ consists in replacing it by two *pinched* halflines on its end vertices v_1 and v_2. It is well defined for all the lines of a graph. On the contrary, the contraction must respect the strand structure and is well defined only for lines $l_{v_1v_2}$ connecting two *different* vertices $v_1 \neq v_2$. The polynomial define by Eq. (3) respects the contraction deletion equation (2)

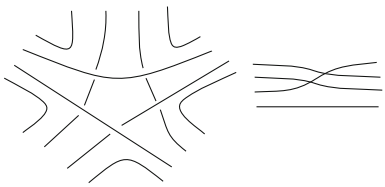

FIGURE 2. GFT vertex and a GFT line in four dimensions

only for such lines. The end graphs (those which cannot be contracted further) consist of connected components with only one vertex, but possibly many lines and faces. The polynomial of such end graphs can be read from Eq. (3).

The crucial property of the topological polynomials is that the definitions in term of subgraphs and the contraction deletion properties can be exchanged. That is, the polynomials of Definitions 1 and 2 are the *unique* solutions of the deletion contraction equation (2) respecting the appropriate forms for the end graphs. Although, given just Eq. (2), one might think that its solution depends on the order in which the lines are contracted (deleted), Eqs. (1) and (3) show that it does not.

3. Colored Group Field Theory Graphs

Ribbon graphs generalize in higher dimensions to group field theory graphs [22–24]. The GFT graphs are generated by a path integral and are built by the following rules.

The GFT vertex in n dimension has coordination $n+1$. Each halfline (and consequently line) has exactly n strands. Inside a vertex, the strands connect two half lines. In n dimensions, if we label the strands of a halfline 1 to n turning *anticlockwise*, the strand p connects to the p'th successor halfline when turning *clockwise* around the vertex. Every GFT line connects two half lines with an arbitrary permutation of the strands.

Figure 2 presents the GFT vertex and a typical GFT line in four dimensions.

The reader can check that a GFT graph in two dimensions is a ribbon graph with vertices of coordination three. As such, it is dual to a triangulation of a two dimensional surface. Considering the ribbon vertices of the graph as 0-cells, its lines as 1-cells and its faces as 2-cells, a ribbon graph becomes a two dimensional cellular complex. One would expect that the GFT graphs in higher dimension also have a cellular complex structure. This is not true in general because the permutations of strands on the lines prevent one from defining cells of dimension higher that two!

A solution is to consider only the colored group field theory graphs introduced in [1]. In fact, to our knowledge, this is the *only* category of graphs generated by a path integral which has an associated complex structure in

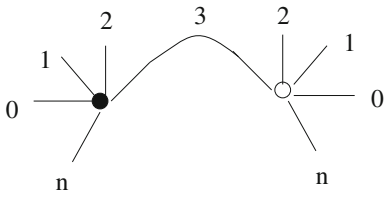

FIGURE 3. Two vertices and a line in a colored graph

arbitrary dimension[3]! The graphs obtained by the perturbative development of the color group field theory action of [1] obey

Definition 3. A CGFT graph in n dimensions is a GFT graph such that

- The CGFT vertices are stranded vertices. The set of vertices $\mathcal{V}(\mathcal{G}) = \{v_1, \dots v_n\}$ is the disjoint union of two sets $\mathcal{V}(\mathcal{G}) = \mathcal{V}^+(\mathcal{G}) \cup \mathcal{V}^-(\mathcal{G})$. $\mathcal{V}^+(\mathcal{G})$ is the set of positive vertices and $\mathcal{V}^-(\mathcal{G})$ is the set of negative vertices.
- The lines $l^i_{v_1 v_2} \in \mathcal{L}(\mathcal{G})$ connect a positive and a negative vertex ($v_1 \in \mathcal{V}^+(\mathcal{G})$ and $v_2 \in \mathcal{V}^-(\mathcal{G})$) and posses a color index $i \in \{0, \dots n\}$. The n strands of all CGFT lines are parallel. Halflines also possess a color index.
- Each color appears exactly once among the lines or halflines touching a vertex. The colors are encountered in the order $0, \dots, n$ when turning clockwise around a positive vertex and anticlockwise around a negative one.

A CGFT graph admits two equivalent representations, either as a stranded graph, or simply as an edge colored graph, obtained by collapsing all the strands belonging to all lines. As the connectivity of strands inside the CGFT vertex and lines are fixed the two representations are in one to one correspondence.

A colored graph is made of colored lines connecting positive and negative vertices. In Fig. 3, the line of color 3 connects the positive vertex on the left with the negative one on the right. Figure 4 gives the two representations for the same graph.

3.1. Bubbles and Cellular Structure

In the definition of the Bollobás–Riordan polynomial the faces (internal and external) played a crucial role. In higher dimensions the faces generalize to higher dimensional cells, called bubbles.

First consider $\mathcal{G}$ a CGFT graph with no external half lines. In [1] we defined the p-cells of $\mathcal{G}$ as

Definition 4. A "p-bubble" with colors $i_1 < \dots < i_p$ of a graph with $n+1$ colors $\mathcal{G}$ with no external halflines is a maximal connected components made of lines of colors $i_1, \dots, i_p$. We denote it $\mathcal{B}^{\mathcal{C}}_{\mathcal{V}}$, where $\mathcal{C} = \{i_1, \dots, i_p\}$ is the ordered set of colors of the lines in the bubbles and $\mathcal{V}$ is the set of vertices.

[3] In three dimensions one also has the alternative to use the orientable model of [32], but this cannot be generalized to higher dimensions.

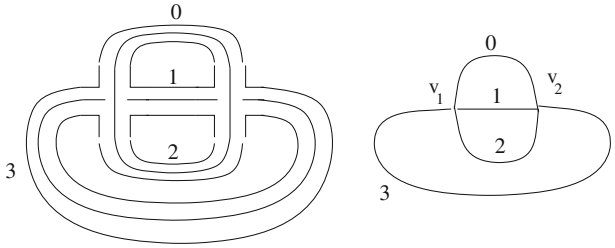

FIGURE 4. A closed colored graph in three dimensions

Note that, unlike the subgraphs of Sect. 2, the connected components *do not* have half lines. For example, for the graph in Fig. 4 we have the 3-bubbles $\mathcal{B}^{012}_{v_1v_2}$, $\mathcal{B}^{013}_{v_1v_2}$, $\mathcal{B}^{023}_{v_1v_2}$ and $\mathcal{B}^{123}_{v_1v_2}$, the 2-bubbles (that is faces) $\mathcal{B}^{01}_{v_1v_2}$, $\mathcal{B}^{02}_{v_1v_2}$, $\mathcal{B}^{03}_{v_1v_2}$, $\mathcal{B}^{12}_{v_1v_2}$, $\mathcal{B}^{13}_{v_1v_2}$, $\mathcal{B}^{23}_{v_1v_2}$, the one bubbles (that is lines) $\mathcal{B}^{0}_{v_1v_2}$, $\mathcal{B}^{1}_{v_1v_2}$, $\mathcal{B}^{2}_{v_1v_2}$, $\mathcal{B}^{3}_{v_1v_2}$, and finally the 0-bubbles (that is vertices) $\mathcal{B}_{v_1}$, $\mathcal{B}_{v_2}$.

Like the graph $\mathcal{G}$, the p-bubbles themselves admit graphical representations either as stranded graphs or as edge colored graphs. For instance in Fig. 4, the stranded graph of the 3-bubble $\mathcal{B}^{012}_{v_1v_2}$ is obtained by deleting all strands belonging to the line $l^3_{v_1v_2}$. Similarly the stranded graph of the 2-bubble $\mathcal{B}^{01}_{v_1v_2}$ is obtained by deleting all strands belonging to the lines $l^2_{v_1v_2}$ and $l^3_{v_1v_2}$.

Considering the representation of bubbles as stranded graphs it is easy to see that in any dimension, the *strands* themselves always correspond to 2-bubbles. This remark is crucial for the next section.

As proved in [1], the p-bubbles define a cellular complex and a cellular homology induced by the boundary operator

Definition 5. The p'th boundary operator d_p acting on a p-bubble $\mathcal{B}^{\mathcal{C}}_{\mathcal{V}}$ with colors $\mathcal{C} = \{i_1, \dots i_p\}$ is

- for $p \geq 2$,

$$d_p(\mathcal{B}^{\mathcal{C}}_{\mathcal{V}}) = \sum_q (-)^{q+1} \sum_{\substack{\mathcal{B}'^{\mathcal{C}'}_{\mathcal{V}'} \in \mathfrak{B}^{p-1} \\ \mathcal{V}' \subset \mathcal{V}\ \mathcal{C}' = \mathcal{C} \setminus i_q}} \mathcal{B}'^{\mathcal{C}'}_{\mathcal{V}'}\ , \tag{4}$$

  which associates to a p-bubble the alternating sum of all $(p-1)$-bubbles formed by subsets of its vertices.
- for $p = 1$, as the lines $\mathcal{B}^i_{v_1v_2}$ connect a positive vertex ($v_1 \in \mathcal{V}^+(\mathcal{G})$) to a negative one, $v_2 \in \mathcal{V}^-(\mathcal{G})$

$$d_1 \mathcal{B}^i_{v_1v_2} = \mathcal{B}_{v_1} - \mathcal{B}_{v_2}. \tag{5}$$

- for $p = 0$, $d_0 \mathcal{B}_v = 0$.

3.2. External Half Lines and the Boundary Complex

A graph $\mathcal{G}$ with external half lines is dual to a topological space with boundary. We will first associate to $\mathcal{G}$ a "boundary graph" $\mathcal{G}_\partial$, dual to a triangulation of the boundary of the topological space and then identify a cellular complex structure for $\mathcal{G}_\partial$.

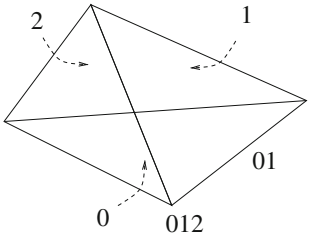

FIGURE 5. Tetrahedron dual to a CGFT vertex

To understand the construction of $\mathcal{G}_\partial$ one needs to consider the topological space dual to $\mathcal{G}$ (see [1] and [32] for details). The dual of a colored graph is essentially a simplicial complex.[4] Each CGFT vertex is dual to a n-simplex Δ^n. The half lines of a vertex are dual to the "sides" of Δ^n, that is the $(n-1)$-simplices Δ^{n-1} bounding it. A boundary simplex Δ^{n-1} inherits the color of the halfline to which it corresponds. The lines (which are identifications of halflines) correspond to the gluing of the two Δ^n simplices along a common Δ^{n-1} boundary simplex. Higher dimensional p-bubbles are dual to $(n-p)$-simplices, in particular the 2-bubbles are dual to Δ^{n-2} simplices. In particular, in the stranded representation of a CGFT graph, the Δ^{n-2} simplices are dual to the strands.

In three dimensions this is represented in Fig. 5. The vertex 0123 is dual to the tetrahedron 0123, the halfline 0 is dual to the triangle 0, the 2-bubble 01 is dual to the edge common to the triangles 0 and 1, and the 3-bubble 012 is dual to the the vertex of the tetrahedron common to the triangles 0, 1, and 2.

If a vertex in a CGFT graph has no half lines then its dual simplex Δ^n sits in the interior of the simplicial complex (in the bulk). On the contrary, if a vertex has half lines, then its dual simplex sits on the boundary of the simplicial complex, and contributes to the triangulation of this boundary with the Δ^{n-1} simplex dual to the half line. The triangulation of the boundary of the simplicial complex is therefore made of all the Δ^{n-1} simplices dual to the halflines of the graph. These Δ^{n-1} simplices are glued along there boundary Δ^{n-2}. The boundary Δ^{n-2} simplices are dual, in the stranded representation of a CGFT graph to the open strands.

To obtain the graph $\mathcal{G}_\partial$ dual to the boundary of the simplicial complex one must draw a vertex for each external halfline of $\mathcal{G}$ and a line for each open strand of $\mathcal{G}$. This can be achieved starting with the stranded representation of the graph $\mathcal{G}$ (see Fig. 6), delete all closed strands, and "pinch" the external strands into a vertex for each external half line. The graph thus obtained is the edge colored representation of $\mathcal{G}_\partial$. We call $\mathcal{G}_\partial$ the "boundary graph" of $\mathcal{G}$.

The vertices of $\mathcal{G}_\partial$ inherit the color of the halfline and the lines of $\mathcal{G}_\partial$ inherit the *couple* of colors of the strand to which they correspond. In the example of Fig. 6, the graph $\mathcal{G}_\partial$ (represented on the right) has one connected

[4] It is in fact a slightly more general gluing of simplices along there faces.

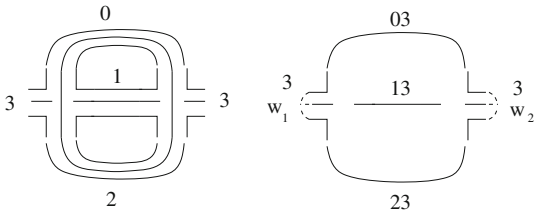

FIGURE 6. A CGFT graph $\mathcal{G}$ and it boundary graph $\mathcal{G}_\partial$

component with two vertices, w_1 and w_2, both of color 3 and three lines of colors 03, 13 and 23.

Note that $\mathcal{G}_\partial$ is a graph of vertices with one color and lines colored by couples of colors: a priori it is very different from a CGFT graph. Nevertheless $\mathcal{G}_\partial$ has a cellular complex structure, strongly reminiscent of the one of $\mathcal{G}$. We denote the set of vertices of $\mathcal{G}_\partial$ (obtained after pinching) by $\mathcal{V}_\partial$. They are the 0-bubbles of the cellular complex of $\mathcal{G}_\partial$. For $p \geq 1$, we have

Definition 6. Let a graph $\mathcal{G}$ and its boundary graph $\mathcal{G}_\partial$ obtained after pinching. For $p \geq 1$ the "boundary p-bubbles" $(\mathcal{B}_\partial)^{\mathcal{C}'}_{\mathcal{V}'_\partial}$ are the maximally connected components of $\mathcal{G}_\partial$ formed by boundary vertices $\mathcal{V}'_\partial \subset \mathcal{V}_\partial$ and boundary lines of colors $i_a i_b$, with $\{i_a, i_b\} \subset \mathcal{C}' \subset \{0, \dots n\}$ and $|\mathcal{C}'| = p+1$.

For example $\mathcal{G}_\partial$ in Fig. 6 has

- 0 bubbles $(\mathcal{B}_\partial)^3_{w_1}$, $(\mathcal{B}_\partial)^3_{w_2}$, which are the vertices of $\mathcal{G}_\partial$.
- 1 bubbles $(\mathcal{B}_\partial)^{03}_{w_1 w_2}$, $(\mathcal{B}_\partial)^{13}_{w_1 w_2}$, $(\mathcal{B}_\partial)^{23}_{w_1 w_2}$, which are the lines of $\mathcal{G}_\partial$.
- 2 bubbles $(\mathcal{B}_\partial)^{013}_{w_1 w_2}$, $(\mathcal{B}_\partial)^{023}_{w_1 w_2}$, $(\mathcal{B}_\partial)^{123}_{w_1 w_2}$, which are the connected components with lines $(03, 13)$, $(03, 23)$ and $(13, 23)$ respectively.

We denote $\mathfrak{B}^p_\partial$ the set of all boundary p-bubbles, and following [1] we define the operator

Definition 7. The p'th boundary operator d^∂_p of the boundary complex, acting on a boundary p-bubble $(\mathcal{B}_\partial)^{\mathcal{C}}_{\mathcal{V}_\partial}$ with colors $\mathcal{C} = \{i_1, \dots i_{p+1}\}$ is

- for $p \geq 1$,

$$d^\partial_p[(\mathcal{B}_\partial)^{\mathcal{C}}_{\mathcal{V}_\partial}] = \sum_q (-)^{q+1} \sum_{\substack{(\mathcal{B}'_\partial)^{\mathcal{C}'}_{\mathcal{V}'_\partial} \in \mathfrak{B}^{p-1}_\partial \\ \mathcal{V}'_\partial \subset \mathcal{V}_\partial \ \mathcal{C}' = \mathcal{C} \setminus i_q}} (\mathcal{B}'_\partial)^{\mathcal{C}'}_{\mathcal{V}'_\partial} , \tag{6}$$

- for $p = 0$, $d^\partial_0[(\mathcal{B}_\partial)^{i_1}_w] = 0$.

For $\mathcal{G}_\partial$ of Fig. 6 for instance,

$$\begin{aligned} d^\partial_2[(\mathcal{B}_\partial)^{013}_{w_1 w_2}] &= (\mathcal{B}_\partial)^{13}_{w_1 w_2} - (\mathcal{B}_\partial)^{03}_{w_1 w_2} \\ d^\partial_1[d^\partial_2[(\mathcal{B}_\partial)^{013}_{w_1 w_2}]] &= (\mathcal{B}_\partial)^3_{w_1} + (\mathcal{B}_\partial)^3_{w_2} - (\mathcal{B}_\partial)^3_{w_1} - (\mathcal{B}_\partial)^3_{w_2} = 0. \end{aligned} \tag{7}$$

The operator d^∂_p is a boundary operator in the sense

Lemma 2.

$$d^{\partial}_{p-1}\circ d^{\partial}_{p}=0. \tag{8}$$

Proof. The proof goes much like its counterpart presented in [1]. Consider the application of two consecutive boundary operators on a boundary p-bubble

$$d^{\partial}_{p-1}d^{\partial}_{p}[(\mathcal{B}_{\partial})^{\mathcal{C}}_{\mathcal{V}_{\partial}}]=\sum_{q}(-)^{q+1}\sum_{\substack{(\mathcal{B}'_{\partial})^{\mathcal{C}'}_{\mathcal{V}'_{\partial}}\in\mathfrak{B}^{p-1}_{\partial}\\ \mathcal{V}'_{\partial}\subset\mathcal{V}_{\partial}\ \mathcal{C}'=\mathcal{C}\setminus i_q}} d^{\partial}_{p-1}[(\mathcal{B}'_{\partial})^{\mathcal{C}'}_{\mathcal{V}'_{\partial}}] \tag{9}$$

$$=\sum_{q}(-)^{q+1}\sum_{\substack{(\mathcal{B}'_{\partial})^{\mathcal{C}'}_{\mathcal{V}'_{\partial}}\in\mathfrak{B}^{p-1}_{\partial}\\ \mathcal{V}'_{\partial}\subset\mathcal{V}_{\partial}\ \mathcal{C}'=\mathcal{C}\setminus i_q}}\Big[\sum_{r<q}(-)^{r+1}\sum_{\substack{(\mathcal{B}''_{\partial})^{\mathcal{C}''}_{\mathcal{V}''_{\partial}}\in\mathfrak{B}^{p-2}_{\partial}\\ \mathcal{V}''_{\partial}\subset\mathcal{V}_{\partial}\ \mathcal{C}''=\mathcal{C}\setminus i_q\setminus i_r}}(\mathcal{B}''_{\partial})^{\mathcal{C}''}_{\mathcal{V}''_{\partial}}$$

$$+\sum_{r>q}(-)^{r}\sum_{\substack{(\mathcal{B}''_{\partial})^{\mathcal{C}''}_{\mathcal{V}''_{\partial}}\in\mathfrak{B}^{p-2}_{\partial}\\ \mathcal{V}''_{\partial}\subset\mathcal{V}_{\partial}\ \mathcal{C}''=\mathcal{C}\setminus i_q\setminus i_r}}(\mathcal{B}''_{\partial})^{\mathcal{C}''}_{\mathcal{V}''_{\partial}}, \tag{10}$$

as i_r is the $r-1$'th color of $\mathcal{C}'\setminus i_q$ if $q<r$. The two terms cancel by exchanging q and r in the second term. □

The boundary bubbles define a cellular complex with attaching maps induced by the boundary operator of Definition 7. With the appropriate substitutions, one reproduces the main results of [1] for the cellular homology of $\mathcal{G}_{\partial}$ defined by d^{∂}_{p}.

Lemma 3. *Let $\mathcal{G}_{\partial}$ a connected boundary CGFT graph with $n+1$ colors. The operator d^{∂}_{p} has the following properties*

- *The d^{∂}_{0} operator respects*

$$\ker(d^{\partial}_{0})=\bigoplus_{|\mathfrak{B}^{0}_{\partial}|}\mathbb{Z}. \tag{11}$$

- *The d^{∂}_{1} operator respects*

$$\ker(d^{\partial}_{1})=\bigoplus_{|\mathfrak{B}^{1}_{\partial}|-|\mathfrak{B}^{0}_{\partial}|+1}\mathbb{Z}\,,\qquad \mathrm{Im}(d^{\partial}_{1})\bigoplus_{|\mathfrak{B}^{0}_{\partial}|-1}\mathbb{Z}. \tag{12}$$

- *The d^{∂}_{n-1} operator respects*

$$\ker(d^{\partial}_{n-1})=\mathbb{Z}\,,\qquad \mathrm{Im}(d^{\partial}_{n-1})\bigoplus_{|\mathcal{B}^{n-1}_{\partial}|-1}\mathbb{Z}. \tag{13}$$

In consequence, for all graphs, denoting the homology groups of $\mathcal{G}_{\partial}$ as H^{∂}_{q}, we have

$$H^{\partial}_{0}=\mathbb{Z},\quad H^{\partial}_{n}=\mathbb{Z}. \tag{14}$$

And if $\mathcal{G}$ is moreover a three dimensional graph (that is it has four colors), then for each connected component of $\mathcal{G}_\partial$ we have

$$H_0^\partial = \mathbb{Z}, \quad H_1^\partial = \bigoplus_{2g} \mathbb{Z}, \quad H_2^\partial = \mathbb{Z}, \tag{15}$$

that is $\mathcal{G}_\partial$ is a union of tori.

4. Topological Polynomials of GFT Graphs

Having at our disposal a good definition of bubbles in arbitrary colored graphs we proceed to generalize the topological polynomials to higher dimensional graphs. However one encounters a problem.

There is an incompatibility between the contraction of lines of Sect. 2 and the colored graphs of Definition 3. If $\mathcal{G}$ is a colored graph and l one of its lines, $\mathcal{G} - l$ is still a colored graph, but $\mathcal{G}/l$ is not. The vertex obtained by identifying the endvertices of l does not respect the conditions of Definition 3. But the p-bubbles are defined only for colored graphs. It is therefore needed to modify the contraction move to ensure that $\mathcal{G}/l$ remains a colored graph. This is achieved by slightly enlarging the class of graphs we consider to graphs with active and passive lines.

Definition 8. A colored graph with active and passive lines is a colored graph $\mathcal{G}$ and a partition of the lines $\mathcal{L}(\mathcal{G})$ into two disjoint sets, $\mathcal{L}(G) = \mathcal{L}_1(\mathcal{G}) \cup \mathcal{L}_2(\mathcal{G})$, such that $\mathcal{L}_2(\mathcal{G})$ is a forest.[5] The lines in the first set, $\mathcal{L}_1(\mathcal{G})$ are called *active* lines whereas the lines in the second set $\mathcal{L}_2(\mathcal{G})$ are called *passive*.

Note that a colored graph with no passive lines is just a colored graph in the sense of Definition 3. For a colored graph with active and passive lines, we define the deletion and contraction *only* for the active lines $l \in \mathcal{L}_1(\mathcal{G})$ as follows

Definition 9. For all active lines $l \in \mathcal{L}_1(\mathcal{G})$ we define

- The graph with the line l deleted, $\mathcal{G} - l$ with $\mathcal{V}(\mathcal{G} - l) = \mathcal{V}(\mathcal{G})$, $\mathcal{L}_1(\mathcal{G} - l) = \mathcal{L}_1(\mathcal{G}) \backslash \{l\}$ and $\mathcal{L}_2(\mathcal{G} - l) = \mathcal{L}_2(\mathcal{G})$.
- The graph with the line l contracted $\mathcal{G}/l$ with $\mathcal{V}(\mathcal{G}/l) = \mathcal{V}(\mathcal{G})$, $\mathcal{L}_1(\mathcal{G}/l) = \mathcal{L}_1(\mathcal{G}) \backslash \{l\}$ and $\mathcal{L}_2(\mathcal{G}/l) = \mathcal{L}_2(\mathcal{G}) \cup \{l\}$.

That is the contraction is reinterpreted as transforming an active lines into a passive one, instead of the identification of the end vertices. The contraction is defined therefore only if $\{l\} \cup \mathcal{L}_2(\mathcal{G})$ is still a forest (that is it has no loops). Note that one can use the new definitions of $\mathcal{G} - l$ and $\mathcal{G}/l$ also for the graphs of Sect. 2. Then Eq. (2) holds for all active lines and Definition 1 holds if $\mathcal{L}_2(\mathcal{G}) = \emptyset$.

Let $\mathcal{G}$ be a CGFT graph with $n+1$ colors, and $\mathcal{G}_\partial$ its boundary graph. As before, let $\mathfrak{B}^p, 0 \leq p \leq n$ be the set of all *bulk* p-cells (defined by Definition 4), and $\mathfrak{B}^p_\partial, 0 \leq p \leq n-1$ the set of *boundary* p-cells (defined by Definition 6).

[5] That is the lines in $\mathcal{L}_2(\mathcal{G})$ do not form loops.

Denote $\mathfrak{B}^{n+1}$ the set of the connected components of $\mathcal{G}$ and $\mathfrak{B}^n_\partial$ the set of connected components of $\mathcal{G}_\partial$. To define the topological polynomial associated to $\mathcal{G}$, we introduce a variable x_p counting all the bulk p-cells and a variable y_p counting all the boundary p-cells. Furthermore, we associate a variable β_l to all active lines in $\mathcal{G}$.

Definition 10. The topological polynomial $P_{\mathcal{G}}(\{\beta_l\},\{x_p\},\{y_p\})$ is

$$P_{\mathcal{G}}(\{\beta_l\},\{x_p\},\{y_p\}) = \sum_{\mathcal{H}\subset\mathcal{G};\mathcal{L}_2(\mathcal{H})=\mathcal{L}_2(\mathcal{G})} \Big(\prod_{l\in\mathcal{L}_1(\mathcal{H})}\beta_l\Big)\prod_{p=0}^{n+1} x_p^{|\mathfrak{B}^p|}\prod_{p=0}^{n} y_p^{|\mathfrak{B}^p_\partial|}. \tag{16}$$

Note that the variables x_0 and x_1 are redundant: the number of vertices of any subgraph is equal to the number of vertices of the initial graph, thus $x_0^{|\mathfrak{B}^0|}$ is just an overall multiplicative factor and x_1 contributes just with a global $x_1^{\mathcal{L}_2(\mathcal{G})}$ multiplicative factor after a uniform rescaling of the line parameters β_l. An explicit example is detailed at length in the Appendix.

The polynomial of Eq. (16) has the following behavior under various rescalings

$$\begin{aligned} P_{\mathcal{G}}(\{\beta_l\},\{\rho^{(-)^p}x_p\},\{\rho^{(-)^{p+1}}y_p\}) &= \rho^{\chi(\mathcal{G})}P_{\mathcal{G}}(\{\beta_l\},\{x_p\},\{y_p\}) \\ P_{\mathcal{G}}(\{\beta_l\},\{x_p\},\{\rho^{(-)^p}y_p\}) &= \rho^{\chi(\mathcal{G}_\partial)}P_{\mathcal{G}}(\{\beta_l\},\{x_p\},\{y_p\}), \end{aligned} \tag{17}$$

with $\chi(\mathcal{G})$ and $\chi(\mathcal{G}_\partial)$ the Euler characteristics of $\mathcal{G}$ and $\mathcal{G}_\partial$ respectively. Moreover it respects the contraction deletion relation

Lemma 4. *For all active lines $l\in\mathcal{L}_1(\mathcal{G})$ such that $\{l\}\cup\mathcal{L}_2(\mathcal{G})$ is a forest*

$$\begin{aligned} P(\{\beta\},\{x_p\},\{y_p\}) = \beta_l P_{\mathcal{G}/l}(\{\beta\}\backslash\{\beta_l\},\{x_p\},\{y_p\}) \\ +P_{\mathcal{G}-l}(\{\beta\}\backslash\{\beta_l\},\{x_p\},\{y_p\}), \end{aligned} \tag{18}$$

Proof. Note that any active line l divides the subgraphs indexing the sum in (16), $\mathcal{H}\subset\mathcal{G}$ with $\mathcal{L}_2(\mathcal{H})=\mathcal{L}_2(\mathcal{G})$, into two families, namely

$$\mathcal{F}_{l\in}(\mathcal{G}) = \{\mathcal{H}|l\in\mathcal{L}_1(\mathcal{H})\} \quad \mathcal{F}_{l\notin}(\mathcal{G}) = \{\mathcal{H}|l\notin\mathcal{L}_1(\mathcal{H})\}. \tag{19}$$

We split (16) into two terms corresponding to these two families. All the subgraphs in the first family contain l, thus we can factor β_l in front of the first term, and reinterpret the line l as a passive line in the graph $\mathcal{H}/l$. The set of graphs $\mathcal{F}_{l\in}(\mathcal{G})$ is in one to one correspondence to the set of all the subgraphs $\mathcal{H}/l\subset\mathcal{G}/l$ with $\mathcal{L}_2(\mathcal{H}/l)=\mathcal{L}_2(\mathcal{G}/l)=\mathcal{L}_2(\mathcal{G})\cup\{l\}$, therefore the first term on the rhs of Eq. (18) is recovered. The graphs in the second family $\mathcal{F}_{l\notin}(\mathcal{G})$ coincide with the subgraphs of $\mathcal{G}-l$, and one recovers the second term in (18). □

The classical Tutte and Bollobás–Riordan polynomials are recovered as limit cases of the higher dimensional polynomial defined here. For the CGFT graphs with three colors (which are trivalent ribbon graphs) Eqs. (16) and (3) imply

$$P(\{\beta\},\{1,1,z,q\},\{1,1,z\}) = V_{\mathcal{G}}(q,\{\beta\},z)\,, \tag{20}$$

and for an arbitrary CGFT with $\mathcal{L}_2(\mathcal{G}) = \emptyset$

$$P(\{\beta\}, \{1, q\}, \{1\}) = Z_{\mathcal{G}}(q, \{\beta\}). \tag{21}$$

5. A Discussion of Universality

Perhaps the most appealing trait of the Bollobás Riordan and Tutte polynomials is their universality, namely the fact that any graph invariant respecting the deletion-contraction equations can be computed starting from them. In the classical case the proof of such a result is lengthy and technical (see [42,43]) and becomes considerably more difficult for multivariate polynomials [50].

The classical proofs of universality [42,43] rely on a classification of the end graphs of the deletion contraction, chord diagrams in [42,43] (referred to as "rosettes" following [46–49] in the sequel). The first core result established in [42,43] is that all chord diagrams can be reduced by topological "rotation about chords" to canonical rosettes. The proof of universality proceeds then by a multi layer analysis over increasingly complex graphs starting with trivial chord diagrams, and proceeding step by step to canonical chord diagrams, arbitrary chord diagrams and finally arbitrary graphs.

In this section we will introduce the first notions needed for such an analysis for the polynomials presented in this paper. The question is much more subtle and difficult than in the ribbon graphs case, and for the moment out of reach. Identifying canonical colored rosettes with, say, four colors is equivalent to a full classification of three dimensional piecewise linear manifolds and pseudomanifolds, an extremely difficult open question in algebraic topology. Even supposing that one would obtain such canonical rosettes (and we emphasize again that we do not expect such a result any time soon), it would still be a highly non trivial problem to generalize the proof of universality of [42].

5.1. Colored Rosettes

In the classical case the rosettes are the end graphs with one vertex (obtained after the contraction of a tree in the graph) decorated by some loop lines (which cannot be contracted further as they start and end on the same vertex). Similarly, for colored graphs the end graphs are made of forests of passive lines $\mathcal{L}_2(\mathcal{G})$ decorated by active lines l, such that $\forall\{l\},\ \{l\} \cup \mathcal{L}_2(\mathcal{G})$ is not a forest.

A connected end graph $\mathcal{G}$ (that is $\mathcal{L}_2(\mathcal{G})$ contains exactly one tree) admits a representation as a *colored rosette* obtained by splitting all lines in $\mathcal{L}_2(\mathcal{G})$ longitudinally into two pieces (leaving the external half lines of the tree on the appropriate sides) inheriting the color of the line, and deforming the closed circuit of the pieces to a circle. A self explanatory graphical representation of this procedure is given in Fig. 7, where the passive lines are dotted and the active ones are solid. Note that the colored rosettes have a natural counterclockwise orientation.

The inverse procedure is also well defined. To obtain the passive tree starting from the rosette one turns around the circle and identifies adjacent

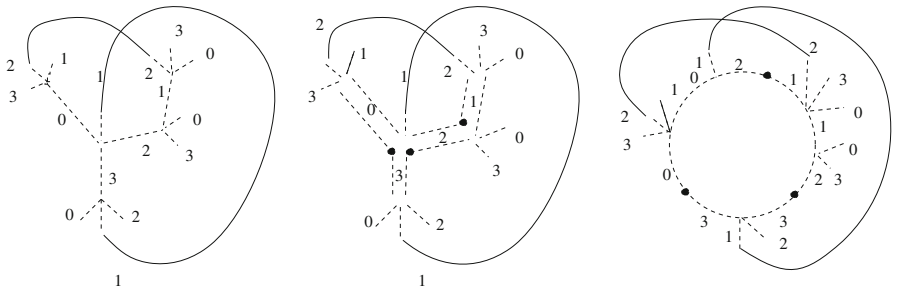

FIGURE 7. Obtaining a colored rosette

pieces having the same color into a tree line. Note that in order to obtain the full passive tree one might need to go around the circle more than once. For the example of Fig. 7 the first pass reconstitutes the lines of colors $0, 1$ and 3 in the passive tree, but one needs a second pass to reconstruct the line of color 2. At first sight the colored rosettes are very similar to the ribbon graphs rosettes, but as the boundary data along the colored rosettes is richer they are noticeably harder to deal with.

The classical proofs of [42,43] proceed by classifying topologically related rosettes. This is achieved by two topological operations, the "rotation about lines" and the "sum of rosettes". We note that there is a slight inconsistency in the definition of the "rotation" in the literature, namely the definition used in [43], is *different* from the one in [42]. It is not clear to us if these two are equivalent, as the definition of [43] imposes some restrictions on "rotations" and, at least at first sight, a "rotation" in the sense of [42] cannot be obtained by a sequence of "rotations" in the sense of [43]. The second topological operation in [42,43], the "sum of rosettes" allows to freely move parts of a rosette with respect to each other, and disentangle complicated rosettes.

In the rest of this section, we will give an appropriate generalization of the "rotation about lines" to colored rosettes. In some cases this operation will allow us to disentangle rosettes, but we will show through counterexamples that this is not generic. Moreover, up to now we have not been able to find an appropriate generalization of the "sum of rosettes" to colored rosettes.

5.2. The R Relation

Following [43] we consider now graphs with two effective vertices separated by at least two lines (that is $\mathcal{L}_2(\mathcal{G})$ has exactly two trees connected by at least two active lines). Contraction of either one or the other of the active lines leads to two distinct rosettes as in Fig. 8 and called R related.

From the point of view of the underlying tree of passive lines, the R relation can be seen as applying the inverse of a contraction move along a line followed by a contraction along another tree line. In the rosette amounts to choose the two pieces on the rosette coming from a passive line (1 in Fig. 8) and identifying them to reconstruct it followed by the split of a newly formed tree line (2 in Fig. 8).

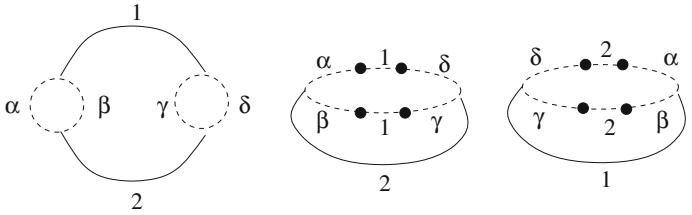

FIGURE 8. R relation

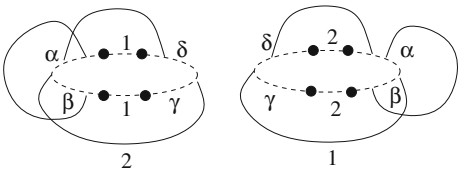

FIGURE 9. Three lines disentangled by an R move

Any line on a rosette separates two different vertices in the colored graph. Call the unique (nonempty) path in the passive tree connecting these two vertices $\mathcal{P}$. On the rosettes, the line lets on the same side (both on the interior or both on the exterior) the two pieces on the rosette coming from the lines in the passive tree *not belonging* to $\mathcal{P}$, and separates on its two sides (one on the interior and one on the exterior of the line) the two pieces on the rosette coming form the lines *belonging* to $\mathcal{P}$. Thus one can perform the R move and exchange the line on the rosette with any one of the lines in $\mathcal{P}$. As the two vertices it connects are of opposing orientation, any line on the rosette encompasses an odd number of pieces, at least one of which comes form $\mathcal{P}$.

In the classical case the rotations allow one to always simplify rosettes with three lines such that at most two intersect. In some cases this holds also for colored rosettes, as is apparent from Fig. 9 (remember that the pieces $\alpha, \beta, \gamma, \delta$ are all oriented counterclockwise and note that the R relation preserves these orientations).

However this is not generic. For the graph of Fig. 10 no R move can disentangle the three lines in the corresponding rosette.

It is thus very difficult to give a full characterization of colored rosettes and define some canonical rosettes to implement the usual proofs of universality. However the language developed here and the notion of colored rosettes should provide clues to a partial characterization of three dimensional manifolds and pseudomanifolds.

6. Conclusion

In this paper, we introduced topological polynomials adapted to CGFT graphs, obeying a deletion contraction equation. To each CGFT graph we associated

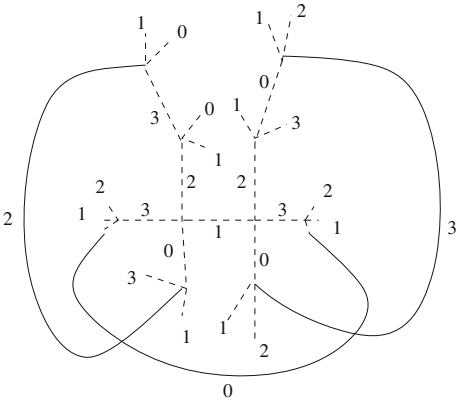

FIGURE 10. Three lines which cannot be disentangled

a boundary graph, and defined and studied its homology. Moreover, in an attempt to address the question of universality of our polynomials we were led to introduce colored rosettes and adapted R moves.

The generalized polynomials reproduce the classical ones for certain values of the parameters. Although the polynomials we define are not the unique generalization one can consider, they already encode nontrivial topological information as seen by the behavior under rescaling of their arguments. One can for instance consider generalizations, in which instead of associating a unique variable x_p which counts all the p-cells, one associates a different variable to each p-cell. Such a polynomial would presumably obey a generalized deletion-contraction for p-cells instead of lines.

Acknowledgements

The author would like to thank Vincent Rivasseau for very useful discussions at an early stage of this work, and an anonymous referee for suggesting the inclusion of the discussion on universality. Research at Perimeter Institute is supported by the Government of Canada through Industry Canada and by the Province of Ontario through the Ministry of Research and Innovation.

Appendix

In this appendix, we detail the topological polynomial and check the contraction deletion relation for the graph in Fig. 4. The subgraphs of this graph are: the total graph formed by the lines 0123, subgraphs with three lines 123, 023, 013, 012, sub graphs with two lines 01, 02, 03, 12, 13, 23, those with one line 0, 1, 2, 3 and the subgraph with zero lines. The polynomial of the complete graph is then

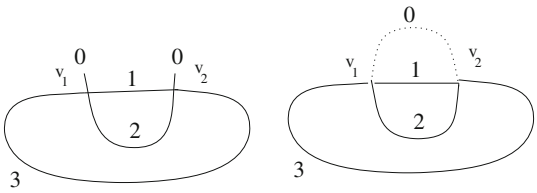

FIGURE 11. The graphs $\mathcal{G} - l$ and $\mathcal{G}/l$

$$\begin{aligned} P_{\mathcal{G}} = {} & \beta_0\beta_1\beta_2\beta_3\ x_0^2x_1^4x_2^6x_3^4x_4 \\ & + (\beta_1\beta_2\beta_3 + \beta_0\beta_2\beta_3 + \beta_0\beta_1\beta_3 + \beta_0\beta_1\beta_2)\ x_0^2x_1^3x_2^3x_3x_4y_0^2y_1^3y_2^3y_3 \\ & + (\beta_0\beta_1 + \beta_0\beta_2 + \beta_0\beta_3 + \beta_1\beta_2 + \beta_1\beta_3 + \beta_2\beta_3)\ x_0^2x_1^2x_2x_4y_0^4y_1^6y_2^4y_3 \\ & + (\beta_0 + \beta_1 + \beta_2 + \beta_3)\ x_0^2x_1x_4y_0^6y_1^9y_2^5y_3 \\ & + x_0^2x_4^2y_0^8y_1^{12}y_2^8y_3^2. \end{aligned} \tag{22}$$

Consider for instance the contributions of the subgraph 012, represented in Fig. 6. It has two vertices, three lines 0, 1 and 2, three internal faces 01, 02 and 12, one internal bubble 012 and one connected component. This yields a factor $x_0^2x_1^3x_2^3x_3x_4$. Its boundary graph is represented on the right hand side of Fig. 6. It has two vertices (both colored 3), three lines colored 03, 13 and 23, three faces, one formed by the lines 01 and 02, another one formed by the lines 01, 03 and the third one formed by the lines 02 and 03, and one connected component, yielding a factor $y_0^2y_1^3y_2^3y_3$. Multiplying the two factors reproduces the coefficient of $\beta_0\beta_1\beta_2$ in Eq. (22)

Chose a line, say 0. The graphs $\mathcal{G} - l$ and $\mathcal{G}/l$ are represented in Fig. 11 where the passive line l_0 of $\mathcal{G}/l$ is represented as a dotted line.

The graph $\mathcal{G} - l$ has subgraphs made of lines 123, 12, 23, 13, 1, 2, 3 and the subgraph with zero lines. Thus

$$\begin{aligned} P_{\mathcal{G}-l} = {} & \beta_1\beta_2\beta_3\ x_0^2x_1^3x_2^3x_3x_4y_0^2y_1^3y_2^3y_3 \\ & + (\beta_1\beta_2 + \beta_1\beta_3 + \beta_2\beta_3)\ x_0^2x_1^2x_2x_4y_0^4y_1^6y_2^4y_3 \\ & + (\beta_1 + \beta_2 + \beta_3)\ x_0^2x_1x_4y_0^6y_1^9y_2^5y_3 \\ & + x_0^2x_4^2y_0^8y_1^{12}y_2^8y_3^2. \end{aligned} \tag{23}$$

All the subgraphs of $\mathcal{G}/l$ will have $l_0 \in \mathcal{L}_2$ as a passive line. They are formed by the active lines 123, 12, 23, 13, 1, 2, 3 and the graph with no active line. Therefore

$$\begin{aligned} P_{\mathcal{G}/l} = {} & \beta_1\beta_2\beta_3\ x_0^2x_1^4x_2^6x_3^4x_4 \\ & + (\beta_2\beta_3 + \beta_1\beta_3 + \beta_1\beta_2)\ x_0^2x_1^3x_2^3x_3x_4y_0^2y_1^3y_2^3y_3 \\ & + (\beta_1 + \beta_2 + \beta_3)\ x_0^2x_1^2x_2x_4y_0^4y_1^6y_2^4y_3 \\ & + x_0^2x_1x_4y_0^6y_1^9y_2^5y_3, \end{aligned} \tag{24}$$

and direct inspection shows that

$$P_{\mathcal{G}} = \beta_0 P_{\mathcal{G}/l} + P_{\mathcal{G}-l}. \tag{25}$$

References

[1] Gurau, R.: Colored group field theory. arXiv:0907.2582 [hep-th]

[2] Nakanishi, N.: Graph Theory and Feynman Integrals. Gordon and Breach, New York (1970)

[3] Itzykson, C., Zuber, J.-B.: Quantum Field Theory. McGraw and Hill, New York (1980)

[4] David, F.: A model of random surfaces with nontrivial critical behavior. Nucl. Phys. B **257**, 543 (1985)

[5] Ginsparg, P.: Matrix models of 2-d gravity. arXiv:hep-th/9112013

[6] Gross, M.: Tensor models and simplicial quantum gravity in >2-D. Nucl. Phys. Proc. Suppl. **25A**, 144–149 (1992)

[7] Sasakura, N.: Tensor model for gravity and orientability of manifold. Mod. Phys. Lett. A **6**, 2613 (1991)

[8] Connes, A.: Noncommutative Geometry. Academic Press Inc., San Diego (1994)

[9] Douglas, M.R., Nekrasov, N.A.: Noncommutative field theory. Rev. Mod. Phys. **73**, 977 (2001). arXiv:hep-th/0106048

[10] Grosse, H., Wulkenhaar, R.: Renormalization of ϕ^4-theory on noncommutative $\mathbb{R}^4$ in the matrix base. Commun. Math. Phys. **256**(2), 305 (2005). arXiv:hep-th/0401128

[11] Grosse, H., Wulkenhaar, R.: Power-counting theorem for non-local matrix models and renormalization. Commun. Math. Phys. **254**(1), 91 (2005). arXiv:hep-th/0305066

[12] Rivasseau, V., Vignes-Tourneret, F., Wulkenhaar, R.: Renormalization of non-commutative ϕ^4-theory by multi-scale analysis. Commun. Math. Phys. **262**, 565 (2006). arXiv:hep-th/0501036

[13] Gurau, R., Magnen, J., Rivasseau, V., Vignes-Tourneret, F.: Renormalization of non-commutative ϕ^4_4 field theory in x space. Commun. Math. Phys. **267**(2), 515 (2006). arXiv:hep-th/0512271

[14] Gurau, R., Magnen, J., Rivasseau, V., Tanasa, A.: A translation-invariant renormalizable non-commutative scalar model. Commun. Math. Phys. **287**, 275 (2009). arXiv:0802.0791 [math-ph]

[15] 't Hooft, G.: A planar diagram theory for strong interactions. Nucl. Phys. B **72**, 461 (1974)

[16] Grosse, H., Wulkenhaar, R.: The beta-function in duality-covariant noncommutative ϕ^4-theory. Eur. Phys. J. **C35**, 277 (2004). arXiv:hep-th/0402093

[17] Disertori, M., Rivasseau, V.: Two and three loops beta function of non commutative phi(4)**4 theory. Eur. Phys. J. C **50**, 661 (2007). arXiv:hep-th/0610224

[18] Disertori, M., Gurau, R., Magnen, J., Rivasseau, V.: Vanishing of beta function of non commutative phi(4)**4 theory to all orders. Phys. Lett. B **649**, 95 (2007). arXiv:hep-th/0612251

[19] Gurau, R., Rosten, O.J.: Wilsonian renormalization of noncommutative scalar field theory. JHEP **0907**, 064 (2009). arXiv:0902.4888 [hep-th]

[20] Geloun, J.B., Gurau, R., Rivasseau, V.: Vanishing beta function for Grosse-Wulkenhaar model in a magnetic field. Phys. Lett. B **671**, 284 (2009). arXiv:0805.4362 [hep-th]

[21] Boulatov, D.: A model of three-dimensional lattice gravity. Mod. Phys. Lett. A **7**, 1629–1646 (1992). arXiv:hep-th/9202074

[22] Freidel, L.: Group field theory: an overview. Int. J. Phys. **44**, 1769–1783 (2005). arXiv:hep-th/0505016

[23] Oriti, D.: Quantum Gravity. In: Fauser, B., Tolksdorf, J., Zeidler, E. (eds.) Birkhauser, Basel (2007). arXiv:gr-qc/0512103

[24] De Pietri, R., Petronio, C.: Feynman diagrams of generalized matrix models and the associated manifolds in dimension 4. J. Math. Phys. **41**, 6671–6688 (2000). arXiv:gr-qc/0004045

[25] Barrett, J., Nash-Guzman, I.: arXiv:0803.3319 (gr-qc)

[26] Engle, J., Pereira, R., Rovelli, C.: The loop-quantum-gravity vertex-amplitude. Phys. Rev. Lett. **99**, 161301 (2007). arXiv:0705.2388

[27] Engle, J., Pereira, R., Rovelli, C.: Flipped spinfoam vertex and loop gravity. Nucl. Phys. B **798**, 251 (2008). arXiv:0708.1236 [gr-qc]

[28] Livine, E.R., Speziale, S.: A new spinfoam vertex for quantum gravity. Phys. Rev. D **76**, 084028 (2007). arXiv:0705.0674 [gr-qc]

[29] Freidel, L., Krasnov, K.: A new spin foam model for 4d gravity. Class. Quant. Grav. **25**, 125018 (2008). arXiv:0708.1595 [gr-qc]

[30] Conrady, F., Freidel, L.: On the semiclassical limit of 4d spin foam models. Phys. Rev. D **78**, 104023 (2008). arXiv:0809.2280 [gr-qc]

[31] Bonzom, V., Livine, E.R., Smerlak, M., Speziale, S.: Towards the graviton from spinfoams: the complete perturbative expansion of the 3d toy model. Nucl. Phys. B **804**, 507 (2008). arXiv:0802.3983 [gr-qc]

[32] Freidel, L., Gurau, R., Oriti, D.: Group field theory renormalization—the 3d case: power counting of divergences. Phys. Rev. D **80**, 044007 (2009). arXiv: 0905.3772 [hep-th]

[33] Magnen, J., Noui, K., Rivasseau, V., Smerlak, M.: arXiv:0906.5477 [hep-th]

[34] Adbesselam, A.: On the volume conjecture for classical spin networks. arXiv: 0904.1734[math.GT]

[35] Geloun, J.B., Magnen, J., Rivasseau, V.: Bosonic Colored Group Field Theory. arXiv:0911.1719 [hep-th]

[36] Kirchhoff, G.: Uber die Auflösung der Gleichungen, auf welche man bei der Untersuchung der linearen Verteilung galvanischer Ströme gefürht wird. Ann. Phys. Chem. **72**, 497–508 (1847)

[37] Tutte, W.T.: Graph Theory. Addison-Wesley, Reading (1984)

[38] 't Hooft, G., Veltman, M.: Regularization and renormalization of gauge fields. Nucl. Phys. **B44**(1), 189–213 (1972)

[39] Crapo, H.H.: The Tutte polynomial. Aequationes Mathematicae **3**, 211–229 (1969)

[40] Sokal, A.: The multivariate Tutte polynomial (alias Potts model) for graphs and matroids, Surveys in combinatorics 2005, pp. 173–226. London Math. Soc. Lecture Note Ser., vol. 327. Cambridge University Press, Cambridge (2005). arXiv:math/0503607

[41] Jackson, B., Procacci, A., Sokal, A.D.: Complex zero-free regions at large $|q|$ for multivariate Tutte polynomials (alias Potts-model partition functions) with general complex edge weights. arXiv:0810.4703v1 [math.CO]

[42] Bollobás, B., Riordan, O.: A polynomial invariant of graphs on orientable surfaces. Proc. Lond. Math. Soc. **83**, 513–531 (2001)

[43] Bollobás, B., Riordan, O.: A polynomial of graphs on surfaces. Math. Ann. **323**, 81–96 (2002)

[44] Ellis-Monaghan, J., Merino, C.: Graph polynomials and their applications. I. The Tutte polynomial. arXiv:0803.3079

[45] Ellis-Monaghan, J., Merino, C.: Graph polynomials and their applications. II. Interrelations and interpretations. arXiv:0806.4699

[46] Gurau, R., Rivasseau, V.: Parametric representation of noncommutative field theory. Commun. Math. Phys. **272**, 811 (2007). arXiv:math-ph/0606030

[47] Rivasseau, V., Tanasa, A.: Parametric representation of 'critical' noncommutative QFT models. Commun. Math. Phys. **279**, 355 (2008). arXiv:math-ph/0701034

[48] Tanasa, A.: Parametric representation of a translation-invariant renormalizable noncommutative model. arXiv:0807.2779 [math-ph]

[49] Krajewski, T., Rivasseau, V., Tanasa, A., Wang, Z.: Topological Graph Polynomials and Quantum Field Theory. Part I. Heat Kernel Theories. arXiv:0811.0186 [math-ph]

[50] Bollobás, B., Riordan, O.: A Tutte polynomial for coloured graphs. Combin. Probab. Comput. **8**, 45–93 (1999)

Razvan Gurau
Perimeter Institute for Theoretical Physics
Waterloo, ON N2L 2Y5, Canada
e-mail: rgurau@perimeterinstitute.ca

Communicated by Carlo Rovelli.

Received: November 16, 2009.

Accepted: April 6, 2010.